

Transition metals activate TFEB in overexpressing cells

Karina A. Peña* and Kirill Kiselyov*¹

*Department of Biological Sciences, University of Pittsburgh, Pittsburgh, PA 15206, U.S.A.

Transition metal toxicity is an important factor in the pathogenesis of numerous human disorders, including neurodegenerative diseases. Lysosomes have emerged as important factors in transition metal toxicity because they handle transition metals via endocytosis, autophagy, absorption from the cytoplasm and exocytosis. Transcription factor EB (TFEB) regulates lysosomal biogenesis and the expression of lysosomal proteins in response to lysosomal and/or metabolic stresses. Since transition metals cause lysosomal dysfunction, we proposed that TFEB may be activated to drive gene expression in response to transition metal exposure and that such activation may influence transition metal toxicity. We found that transition metals copper (Cu) and iron (Fe) activate recombinant TFEB and stimulate the expression of TFEB-dependent genes in TFEB-overexpressing cells. In cells

that show robust lysosomal exocytosis, TFEB was cytoprotective at moderate levels of Cu exposure, decreasing oxidative stress as reported by the expression of heme oxygenase-1 (*HMOX1*) gene. However, at high levels of Cu exposure, particularly in cells with low levels of lysosomal exocytosis, activation of overexpressed TFEB was toxic, increasing oxidative stress and mitochondrial damage. Based on these data, we conclude that TFEB-driven gene network is a component of the cellular response to transition metals. These data suggest limitations and disadvantages of TFEB overexpression as a therapeutic approach.

Key words: copper, lysosomes, transcription factor, transcription factor EB (TFEB), transition metals.

INTRODUCTION

Low levels of transition metals, such as Cu and Fe, are essential to carry out several functions in the cell; however, exposure to high levels of these metals can be detrimental [1]. High dietary uptake or inhalation of transition metals causes conditions such as cirrhosis and dementia [2]. The loss of cellular components involved in the regulation of transition metals homeostasis results in metal overload and is a root cause of several human diseases, such as Wilson's and Menkes diseases [3–5]. Beyond that, transition metals are key factors in the pathogenesis of stroke, Alzheimer's and Parkinson's diseases, among others [1,6–13]. In fact, accumulation of transition metals is thought to cause neurodegeneration through the production of reactive oxygen species (ROS) catalysed by transition metals [14–16]. Thus, the use of metal and ROS chelation is considered a treatment option for neurodegenerative diseases [9].

Metals enter the cell through plasma membrane transporters [17,18] and by endocytosis of free and protein-bound metals [19], which may enter the endocytic pathway non-specifically or bound to specific receptors, as is the case for the transport of Fe-bound transferrin through binding to transferrin receptor [17,18]. Metals separate from the binding proteins in the lower endocytic pathway, due to low pH and proteolytic activity present in these compartments. Autophagy of metal-bound proteins is another means of transition metal delivery into the lysosomes. An alternative pathway of metal entry into the lysosomes is through metal transporters present in membranes of intracellular organelles, including lysosomes. These transporters play an important role in evacuating potentially toxic metals from the cytoplasm into intracellular organelles. Indeed lysosomal uptake and exocytosis of Zn is critical for its detoxification [20]. Confocal immunohistochemistry and subcellular fractionation

suggest the presence of Zn transporters ZnT2 and ZnT4 in the lysosomal membrane, at least under certain conditions [21,22]. Their suppression or overexpression causes general and lysosomal Zn mishandling [21,23,24]. Similar evidence exists for Cu as well, since proteomic analysis confirms localization of ATP7B in the lysosomal membranes [25,26]. Recently published data show that Cu absorption from the cytoplasm into the lysosomes through ATP7B is followed by Cu clearance via lysosomal exocytosis [27]. Our recently published data show that brief exposure to Cu activates lysosomal exocytosis to facilitate the expulsion of this metal [28]. Based on this evidence, lysosomes appear to serve as a cellular metal sink that absorbs and detoxifies transition metals.

The removal of transition metals from the lysosomes is a function of ion transporters, best characterized of which is divalent metal transporter 1 (DMT1) (SLC11A2) [29]. Among other metal transporters implicated in this process is transient receptor potential mucolipin-1 (TRPML1), whose loss appears to affect the distribution of Zn and Fe between the lysosomes and the cytoplasm [21,30–32]. Lysosomal exocytosis has emerged as a key mechanism of Zn and Cu removal [20,27,28]. If metal delivery to the lysosomes exceeds its clearance, as is likely to happen during high-dietary metal uptake, metals build up in the lysosomes. Although the account of metal effect in lysosomes is far from being complete, it is clear that the ensuing lysosomal deficiencies can be explained by direct inhibition of the lysosomal enzymes and transporters by transition metals and by ROS-mediated formation of lipofuscin. The detrimental effect of transition metals on the lysosomes suggests that, at least under certain conditions, lysosomes themselves are a target of transition metal toxicity.

The expression of the components that regulate lysosomal function is under the control of transcription factor EB (TFEB)

Abbreviations: CCCP, carbonyl cyanide *m*-chlorophenylhydrazine; CCS, copper chaperone to superoxide dismutase; CLEAR, co-ordinated lysosomal expression and regulation; CTS, cathepsin; GAPDH, glyceraldehyde-3-phosphate dehydrogenase; HEK, human embryonic kidney; HMOX1, heme oxygenase-1; HRP, horseradish peroxidase; mTORC1, mammalian target of rapamycin complex 1; qPCR, quantitative PCR; ROS, reactive oxygen species; TFEB, transcription factor EB; ZnT, Zn transporter; β -Hex, β -hexosaminidase.

¹ To whom correspondence should be addressed (email kiselyov@pitt.edu).

and its relatives such as TFE3 [33–36]. TFE3 binds to the promoter regions of genes containing the co-ordinated lysosomal expression and regulation (CLEAR) element [33,36,37] and has been indicated as a master regulator of lysosomal biogenesis and autophagy. These transcription factors are regulated by mammalian target of rapamycin complex 1 (mTORC1), which senses lysosomal status and nutrient availability and regulates protein synthesis and autophagy [38–40]. Under normal conditions (low lysosomal pH and high nutrients), TFE3 is inactivated by mTORC1-dependent phosphorylation, leading to 14-3-3 binding and retention of TFE3 in the cytoplasm [39]. Inhibition of mTORC1 leads to an increase in the dephosphorylated form of TFE3 and its translocation to the nucleus. In the nucleus, TFE3 promotes the activation of a set of genes driving lysosomal function and autophagy including genes coding for lysosomal hydrolases such as cathepsin B and cathepsin D (*CTSB* and *CTSD* respectively), structural proteins such as lysosomal-associated membrane protein 1 Lamp1 (*LAMP1*) and many others [33,36,37]. This feedback loop, mediated by TFE3, up-regulates lysosomal and autophagic activity in response to metabolic cues. The fact that up-regulation of the TFE3-driven gene network was demonstrated in lysosomal storage disorders and can be induced by lysosomal inhibitors suggests that deficits of the lysosomal function are reported through this gene network as well.

TFE3 overexpression has been recently used to correct cellular and tissue pathologies in a range of diseases including Huntington's and Parkinson's diseases [37,41–43]. Such an effect can be explained by TFE3-induced stimulation of various aspects of the lysosomal function, including lysosomal exocytosis that may compensate or correct the abnormalities underlying these conditions. It is unclear whether this principle is universal. Indeed, one can argue that under certain condition, making more lysosomes may enhance the effects of the toxin. This idea finds support in the recent evidence of increased cancer drug retention in the lysosomes of TFE3-overexpressing cells [44]. In the course of the present studies, we sought to answer whether TFE3 senses the lysosomal deficiencies caused by transition metals, particularly Cu. We found that transition metal exposure activates overexpressed TFE3, increasing the expression of lysosomal genes. Although this effect was cytoprotective at moderate Cu exposure, at high levels of Cu exposure it was associated with increased oxidative stress and mitochondrial damage, which were especially pronounced in cells with low levels of lysosomal exocytosis. The central conclusion from our studies is that cytoprotective function of TFE3 requires robust lysosomal exocytosis, in the absence of which TFE3 activation may become toxic. Together, these findings identify TFE3 as a player in the response to transition metal toxicity and suggest that under some conditions, the effects of TFE3 overexpression may enhance toxicity.

EXPERIMENTAL

Cell culture

HEK-293 cells were maintained in DMEM (Dulbecco's modified Eagle's medium; Lonza) supplemented with 10% FBS (Atlanta Biologicals; growth medium) at 37 °C in the presence of 5% CO₂. For metal treatments, cells were incubated either with 100 μM CuCl₂ or with 100 μM FeCl₂ for 24–48 h in growth medium. For sucrose treatment, cells were incubated in growth medium supplemented with 100 mM sucrose for 48 h. Control cells were left untreated. In some experiments, 2 mM glutathione was used.

cDNA transfection

pCMV-TFE3-3×FLAG plasmid was a gift from Dr Rosa Puertollano (NIH). Cells were transfected using Lipofectamine 2000 (Invitrogen). Transfections were performed as described by the manufacturer's protocol. Briefly, cells were seeded at subconfluency and transfected next day either with pCMV-TFE3-3×FLAG (TFE3) or with empty pcDNA3 vector (mock). Media were changed 16–24 h later. In our hands, transfection efficiency exceeded 80%.

Reverse transcriptase and quantitative PCR

For quantitative PCR (qPCR) assays, cells were seeded in 12-well plates, transfected and treated as indicated. Total RNA was isolated from human embryonic kidney (HEK)-293 cells using TRIzol (Invitrogen) according to the manufacturer's protocol. cDNA was synthesized with murine leukaemia virus (MuLV) reverse transcriptase (Applied Biosystems) using 2 μg of total RNA and 0.5 μg of oligo(dT)₁₈ (IDT) as primer. qPCR was carried out using 1:500 dilutions of cDNA, 2× SYBR Green (Fermentas) and 4 μM primer mix per 10 μl of reaction mixture. For gene expression analysis, the following primers (IDT) were used: *CSTD*, forward 5'-GCTGATTCAGGGCGAGTACATGAT-3' and reverse 5'-TGCGACACCTTGAGCGTGTA-3'; *LAMP1*, forward 5'-GGACAACACGACGGTGACAAG-3' and reverse 5'-GAACTTGCATTCATCCCGAACTGGA-3'; *HMOX1*, forward 5'-GAGACGGCTTCAAGCTGGTGAT-3' and reverse 5'-CCGTACCAGAAGGCCAGGTC-3'; *SOD1*, forward 5'-CAAAGTAGAAGAGAGGCATGT-3' and reverse 5'-CTTCAATAGACACATCGGCCA-3'; and *RPL32*, forward 5'-CAACATTGGTTATGGAAGCAACA-3' and reverse 5'-TGACGTTGTGGACCAGGA-3'. *CTSB* primers were obtained from QuantiTect Primer Assay (QT00088641, Qiagen). To ensure amplification of cDNA only, all primers were designed to span exons and negative RT reactions were performed as control. The relative quantification method on the 7300 Real Time System (Applied Biosystems) was used to perform qPCR. Samples were amplified with the following program: 2 min at 50 °C, 10 min at 95 °C and 40 cycles at 95 °C for 15 s followed by 60 °C for 1 min. Samples were run in triplicates. At least three biological replicates were performed per condition. Relative gene expression was calculated using the $\Delta\Delta C_t$ method, where C_t represents the cycle threshold. ΔC_t values were calculated as the difference between the target genes and the expression of the endogenous gene *RPL32* and $\Delta\Delta C_t$ values were calculated relative to untreated controls. Data are presented as fold increase.

Nuclear extraction

Nuclear fractions were prepared as previously described [38]. Briefly, cells were grown in 60 mm dishes, transfected and treated as indicated. Cells were washed two times with 1× ice-cold PBS and transferred to a microcentrifuge tube. Cell suspensions were centrifuged at 300 g for 5 min at 4 °C. Cell pellets were resuspended in NP-40 lysis buffer [10 mM Tris, pH 7.9, 140 mM KCl, 5 mM MgCl₂, 1 mM DTT, 0.5% (v/v) NP-40] supplemented with phosphatase inhibitors (1 mM Na₃VO₄, 1 mM NaF, 100 μM β-glycerophosphate) and protease inhibitors (Protease Inhibitor Cocktail III, Calbiochem) and incubated for 15 min on ice. Cytoplasmic fractions were obtained by centrifuging lysed samples at 1000 g for 5 min at 4 °C. Nuclear pellets were washed two times with NP-40 lysis buffer and resuspended in nuclear lysis buffer [25 mM Tris, pH 7.4, 0.5% (v/v) Triton X-100, 0.5% (w/v) SDS] supplemented with phosphatase and protease

inhibitors. Nuclear fractions were sonicated three times for 10 s each. Cytoplasmic and nuclear fractions were incubated for 5 min at 100 °C in 2× Laemmli sample buffer (BioRad). Samples were loaded on a 10% precast TGX polyacrylamide gel (BioRad) and run at 250 V for 40 min. Proteins were transferred to nitrocellulose membrane (BioRad). Nitrocellulose membranes were blocked in 10% milk in Tris-Buffered Saline and Tween 20 (TBS-T) for 1 h. All primary antibodies were incubated overnight at 4 °C in 1% milk in TBS-T. To detect TFEB-3×FLAG, mouse anti-FLAG antibody (M5, Sigma) was used at 1:2000 dilution. For GAPDH (glyceraldehyde-3-phosphate dehydrogenase), rabbit anti-GAPDH antibody was used at 1:20000 dilution. Horseradish peroxidase (HRP)-conjugated goat anti-mouse or anti-rabbit secondary antibodies (Amersham) were used at 1:20000 and 1:1500 dilution respectively.

Western blot assays

For CCS (copper chaperone to superoxide dismutase) Western blot, cells were grown on six-well plates, transfected and treated with the specified compounds. Cells were washed once with ice-cold 1× PBS. Lysis buffer [20 mM Hepes, pH 7.4, 75 mM NaCl, 1.5 mM MgCl₂, 2 mM EGTA, 2 mM DTT and 0.5% (v/v) Triton-X100], supplemented with protease and phosphatase inhibitors, was added to each well and cells were incubated for 1 h at 4 °C on a shaker. Cells were scraped, transferred to a tube and centrifuged at 16000 g for 10 min at 4 °C. Supernatant was collected and equal amounts of protein per condition were incubated at 100 °C for 5 min in 2× Laemmli sample buffer (BioRad). Samples were loaded on a 12% TGX polyacrylamide gel (BioRad), run at 250 V for 40 min and transferred to PVDF membrane (Millipore). Rabbit anti-CCS antibody was a kind gift from Dr Dennis Thiele. HRP-conjugated anti-rabbit secondary antibody was incubated for 1 h at room temperature. Immunodetection was performed with the Luminata Forte HRP substrate (Millipore). Band densities were measured using ImageJ (NIH). For LC3 detection, rabbit anti-LC3 antibody was used. HRP-conjugated anti-rabbit secondary antibody was incubated for 1 h at room temperature. Immunodetection was performed with the Luminata Forte HRP substrate (Millipore). Band densities were measured using ImageJ.

Microscopy

For confocal microscopy, cells were seeded on coverslips and loaded with LysoTracker Red (Invitrogen) for 15 min at 37 °C in a regular buffer (10 mM Hepes, pH 7.4, 150 mM NaCl, 5 mM KCl, 1 mM CaCl₂, 1 mM MgCl₂, 1 g/l glucose). Hoechst dye was added to the cells for 5 min. Cells were washed once and kept in regular buffer before imaging. Confocal microscopy was performed on the stage of a Leica TCS SP5 confocal microscope, using the 561 nm laser line for LysoTracker Red and the 405 nm laser line for Hoechst dye. Laser intensity and gain were kept the same for all images.

LysoTracker quantification

To analyse LysoTracker images, ImageJ software (NIH) was used. To determine the size of lysosomes, threshold was applied to eight-bit images. Binary images were created and the watershed process was used to separate particles at very close proximity. The particle analysis tool was used to quantify the size and number of individual lysosomes. Particles with an area smaller than 1 μm² were excluded because they may represent slices of lysosomes instead of whole lysosomes. To quantify aggregation of

lysosomes, watershed was not applied to binary images, avoiding the separation of lysosomal complexes. Particles larger than 7 μm² were considered aggregations of three or more lysosomes. Quantification data were plotted using GraphPad Prism software.

JC-1 assay

In order to assess for mitochondrial health, we measured mitochondrial membrane potential using the potential-sensitive dye JC-1 (Invitrogen). JC-1 assays were performed as previously described [30]. Briefly, cells plated on a six-well plate were transfected with either TFEB-3×FLAG or empty vector and treated with CuCl₂ for 48 h at the indicated concentrations. Cells were loaded for 30 min at 37 °C with 1:1000 dilution of JC-1 in growth medium. Cells were rinsed twice with growth medium and 0.05% trypsin (Invitrogen) was added to detach cells. Cells were then pelleted at 300 g for 5 min and were rinsed twice with ice-cold PBS. Cell pellets were resuspended in regular buffer (10 mM Hepes, pH 7.4, 150 mM NaCl, 5 mM KCl, 1 mM CaCl₂, 1 mM MgCl₂, 1 g/l glucose) and measurements were recorded at 485/530 nm for green and 535/590 nm for red, using a fluorometer. Carbonyl cyanide *m*-chlorophenylhydrazone (CCCP) was used as a positive control.

β-Hexosaminidase activity assay

HeLa cells on 12-well plates were treated as indicated. The day of the experiment, cells were washed once with regular buffer and 250 μl of buffer was added to each well. Buffer was collected at the indicated times and incubated with 300 μl of 3 mM 4-nitrophenyl *N*-acetyl-β-D-glucosaminide (N9376, Sigma-Aldrich) for 30 min at 37 °C in 0.1 M citrate buffer (0.1 M sodium citrate, 0.1 M citric acid, pH 4.5). Reactions were stopped by adding 650 μl of borate buffer (100 mM boric acid, 75 mM NaCl, 25 mM sodium borate, pH 9.8) and the absorbance was measured in a spectrophotometer at 405 nm. To determine total cellular content of β-hexosaminidase, cells were lysed with 250 μl of 1% Triton X-100 in PBS and after a 10000 g spin for 5 min at 4 °C; 25 μl of the cell extracts were used for the enzyme activity reaction. Enzyme activity was determined as the amount of 4-nitrophenol produced. Absorbance was calibrated with different amounts of 4-nitrophenol (N7660, Sigma-Aldrich) in 0.1 M citrate buffer.

Statistical significance was calculated using a one-tailed, unpaired *t* test with *P* < 0.05 considered significant. Data are presented as mean ± S.E.M.

RESULTS

Activation of recombinant TFEB and expression of lysosomal genes in cells treated with Cu

The activation of TFEB has been linked to many factors that induce lysosomal stress. Lysosomes play an important role in transition metal homeostasis and thus we reasoned that lysosomal stress could be induced by metal overload, since lysosomal storage disease phenotype was reported in some models of Cu exposure [45]. Lysosomal stress activates TFEB by suppressing its phosphorylation by mTORC1. To test TFEB activation, we used mock- and TFEB-3×FLAG-transfected HEK-293 cells; 24- or 48-h-long exposure to 100 mM sucrose was used as a positive control for TFEB activation [33]. This system provides excellent resolution of TFEB activation details and dynamics. Figure 1(A) shows Western blot analysis of cytoplasmic and nuclear fractions of TFEB-3×FLAG transfected

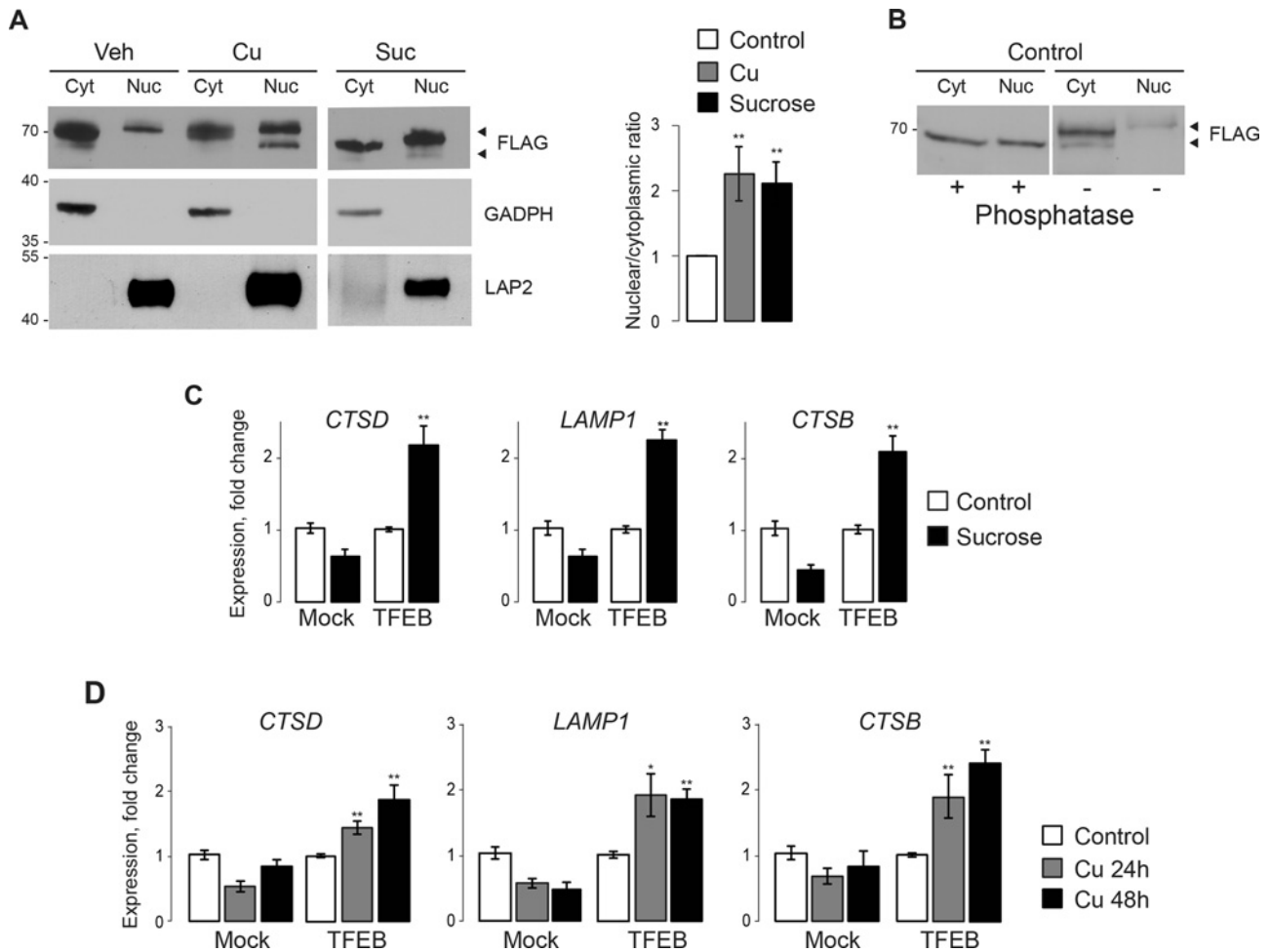


Figure 1 Cu induces TFEB activation

(A) Western blot analysis of nuclear/cytoplasmic fractionation of TFEB cells treated with either 100 μ M CuCl_2 or 100 mM sucrose for 48 h. FLAG antibody was used to detect TFEB-3 \times FLAG; GAPDH and Lamina-associated polypeptide 2 (LAP2) antibodies were used as cytoplasmic and nuclear markers respectively. Image is representative of three independent experiments. The quantification of these experiments is represented in the histogram. (B) Western blot analysis showing the effect of lambda phosphatase on TFEB motility, indicative of TFEB dephosphorylation in Cu-treated cells. (C and D) qPCR analysis of mock and TFEB cells treated with either 100 mM sucrose for 48 h (C) or 100 μ M CuCl_2 for 24 or 48 h (D). Both sucrose and Cu activate the expression of TFEB-regulated genes *CTSB*, *CTSD* and *LAMP1*. Values represented as mean \pm S.E.M. of 3–4 independent experiments; statistical significance was calculated using a two-tailed, unpaired *t* test with $P < 0.05$ (*) and $P < 0.01$ (**) considered significant.

HEK-293 cells. Under control conditions, TFEB is predominantly phosphorylated and concentrated in the cytoplasmic fraction and the nuclear fraction contained relatively low levels of phosphorylated TFEB (lanes 1 and 2 respectively; TFEB phosphorylation status was confirmed using lambda phosphatase; Figure 1B). Exposure of HEK-293 cells to 100 μ M CuCl_2 resulted in the appearance of a fast migrating band in the nuclear fraction (Figure 1A, lane 4), indicating that dephosphorylated TFEB has been translocated to the nucleus of Cu-treated cells. This was confirmed, as in cells treated with 100 mM sucrose TFEB is dephosphorylated in both cytoplasmic and nuclear fractions and TFEB is more abundant in the nuclear fraction (Figure 1A, lanes 5 and 6). Together, these data indicate that Cu exposure is associated with activation of recombinant TFEB: it causes TFEB dephosphorylation and consequent nuclear translocation, which, in turn, results in increased expression levels of lysosomal genes in response to Cu exposure.

TFEB activation should result in an increased expression of the CLEAR network genes. mRNA levels of genes previously assigned to the CLEAR network: *CTSD*, *LAMP1* and *CTSB*,

were analysed using qPCR. In accordance with the previously published results where recombinant TFEB was used to show activation [33,34,36], the normal levels of TFEB in HEK-293 cells seem to be insufficient to cause a measurable response: when 48-h-long exposure to 100 mM sucrose was used as a positive control as before [33], a decrease in *CTSD*, *LAMP1* or *CTSB* mRNA was detected. However, when TFEB-3 \times FLAG was transiently expressed in HEK-293 cells, the expression of *CTSD*, *LAMP1* and *CTSB* genes was significantly increased by the sucrose treatment (Figure 1C; 2.17 ± 0.27 -, 2.24 ± 0.13 -, 2.07 ± 0.29 -fold increase respectively; mean \pm S.E.M. of 3–4 independent experiments). In addition, nutrient starvation stimulated the expression of lysosomal genes in a TFEB-dependent manner (Supplementary Figure S1A). In some experiments, TFEB-overexpressing cells showed increased basal expression of these genes. qPCR readouts presented in Figure 1 are normalized to the basal mRNA levels in mock- and TFEB-transfected cells. Cells transfected with an empty vector did not show an increase in mRNA levels of these genes in response to sucrose (Figure 1C), indicating that the response to sucrose is specific to TFEB expression.

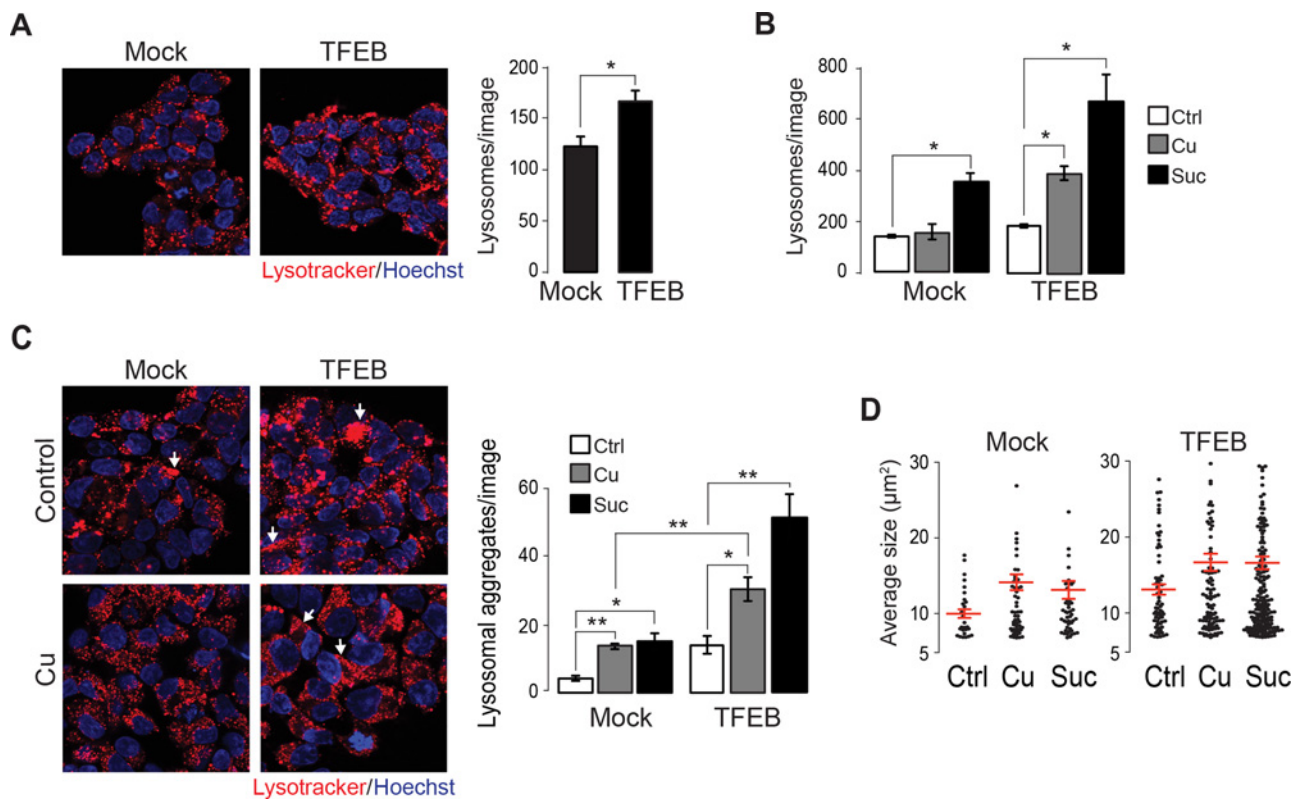


Figure 2 Cu induces aggregation of lysosomes

(A) HEK-293 cells were transiently transfected with TFEB-3×FLAG (TFEB) or an empty vector (mock) and lysosomes were stained with LysoTracker (red) and Hoechst dye was used to stain nucleus (blue). Graph represents the number of individual lysosomes per image analysed as discussed in the text and in Supplementary Figure S3. (B) The number of individual lysosomes is increased in TFEB cells treated with 100 μM CuCl_2 for 24 h or with 100 mM sucrose for 24 h. (C) Confocal images of mock and TFEB cells treated with 100 μM CuCl_2 or 100 mM sucrose stained with lysostracker (red) and Hoechst dye (blue). Arrows indicate lysosomal aggregation. Graph represents the number of lysosomal aggregates per image. (D) Distribution of the size of lysosomal aggregates (in μm^2) of mock and TFEB cells treated with either CuCl_2 or sucrose analysed as in the text and in Supplementary Figure S3. Red lines represent the mean value \pm S.E.M. for each condition. All images were analysed using ImageJ. Values represented as mean \pm S.E.M. of two independent experiments, six images total; statistical significance was calculated using a two-tailed, unpaired *t* test with $P < 0.05$ (*) and $P < 0.01$ (**). (***) considered significant.

Figure 1(D) shows that exposure of mock-transfected HEK-293 cells to 100 μM CuCl_2 for 24 or 48 h did not increase the expression of these CLEAR network genes; indeed, a decrease in corresponding mRNA was detected. However, TFEB-overexpressing cells showed a significant increase in *LAMP1*, *CTSB* and *CTSD* mRNA when cells were treated with Cu for 24 h (1.92 ± 0.33 -, 1.91 ± 0.33 -, 1.45 ± 0.10 -fold increase respectively; 3–4 independent experiments) or 48 h (1.98 ± 0.16 -, 2.4 ± 0.20 -, 1.87 ± 0.23 -fold increase respectively; 3–4 independent experiments). This Cu concentration is within the range commonly used to study Cu transport and toxicity [27,28,46]. Exposure of TFEB cells to another transition metal, 100 μM FeCl_2 also resulted in an increased expression of lysosomal genes (Supplementary Figure S1B). TFE3, a TFEB relative that has been shown to regulate the expression of lysosomal genes [35,47], seems to be activated by Cu as well. Supplementary Figure S1(C) shows that similar to TFEB, TFE3 overexpression prevented the decrease in expression of *LAMP1*, *CTSB* and *CTSD* in response to Cu; however, the magnitude of the increase was smaller than the one observed in TFEB-transfected cells. These data suggest that a TFEB-dependent (and probably TFE3-dependent) mechanism mediates activation of the CLEAR network genes in response to transition metals. Thus, we sought to investigate how the exposure to Cu affects the lysosomal compartment in HEK-293 cells transfected with either a TFEB or an empty vector (mock).

In the next set of experiments, cells were exposed to 100 μM CuCl_2 for 24 h and acidic organelles, including lysosomes, were stained with LysoTracker Red followed by confocal live cell imaging (Figure 2). In order to quantify LysoTracker-positive vesicles, we used a protocol that allows us to distinguish between clustered and individual lysosomes (see ‘Experimental’ section and Supplementary Figure S2). Image analysis revealed that TFEB-transfected cells have a significantly higher number of lysosomes than mock-transfected cells (Figure 2A; 165.3 ± 6.3 compared with 122.0 ± 5.6 lysosomes per image, respectively; two separate experiments, three images each; $P < 0.01$), ostensibly due to increased TFEB-driven lysosomal biogenesis. When cells were treated with Cu, the number of lysosomes was not affected in mock cells, but it was significantly increased in TFEB-transfected cells (Figure 2B; count increased to 353.7 ± 25.21 lysosomes per image; two separate experiments, three images each; $P < 0.01$ when compared with TFEB-transfected, untreated cells). Incubation with 100 mM sucrose, which has been previously described as a lysosomal stressor and TFEB activator [33], was also able to increase the number of lysosomes in both mock and TFEB-transfected cells (Figure 2B). Cu-treated cells showed an increased number of lysosomal aggregates (Figure 2C). Interestingly, the number of Cu-induced lysosomal aggregates was increased by TFEB-overexpression (Figures 2C and 2D; 14 ± 0.58 and 30.67 ± 3.33 aggregates per image in mock and TFEB cells treated with Cu respectively; two separate

experiments, three images each; $P < 0.01$). These data indicate that Cu causes the reorganization of lysosomes by inducing their aggregation and this effect is exacerbated by the overexpression of TFEB.

In addition to changes in lysosomal number and organization in response to Cu, we observed effects on autophagy. We analysed the levels of autophagosome-bound LC3-II by Western blot (Supplementary Figures S3A and S3B). TFEB-transfected HEK-293 cells exposed to Cu showed an increased LC3-II–LC3-I ratio, indicating a higher number of autophagosomes in response to Cu.

In summary, three functional readouts: gene expression, lysosomal build-up and autophagic markers confirm activation of recombinant TFEB by Cu in this system.

The impact of TFEB on Cu-induced oxidative stress

TFEB overexpression has been proposed to be therapeutic in models of several diseases including Huntington's, Parkinson's and Pompe diseases [37,41–43], ostensibly due to activation of lysosomal biogenesis and clearance. Transition metals catalyse the formation of ROS through Fenton reactions favoured by the acidic lysosomal environment [48]. ROS damage lysosomal membranes, probably causing the release of lysosomal digestive enzymes and cell death [49]. High levels of ROS can cause the formation of lipofuscin as a consequence of peroxidation of non-degraded material and impair autophagy [48]. Since lysosomes handle Cu and other transition metals including Fe and Zn [20,21,27,30,31,50–52], we sought to answer whether increases in Cu retention in the lysosomes of TFEB-overexpressing cells increase its toxicity by increasing ROS production. Transition metal toxicity is a factor in cell death in many conditions, including neurodegenerative diseases [4,6,8,53–65], the very conditions against which TFEB overexpression was proposed to be protective.

In order to measure ROS production, we analysed the expression of *HMOX1* gene, which codes for the enzyme called haeme oxygenase-1. *HMOX1* expression is induced by ROS via the NRF2 (nuclear factor (erythroid-derived 2)-like 2) transcription factor that binds to an antioxidant response element (ARE) on the *HMOX1* promoter. As an additional control, in some experiments, we used gene *SOD1* coding for superoxide dismutase, which is activated by metal regulatory transcription factor 1 (MTF-1) [66]. Figure 3(A) shows the results of qPCR analysis for *HMOX1* in TFEB and mock transfected HEK-293 cells after 24 or 48 h treatment with 100 μM CuCl_2 . In both cases, mock-transfected cells showed significant increase in *HMOX1* expression after Cu exposure for 24 h (2.44 ± 0.67 -fold increase, three independent experiments) and 48 h (2.87 ± 0.47 fold increase; three independent experiments). HEK-293 cells expressing TFEB showed an even larger *HMOX1* response: we detected a 4.28 ± 0.58 -fold increase after 24 h and a 6.99 ± 0.99 -fold increase after 48 h (t test $P < 0.01$, $n=3$, Figure 3A). *SOD1* response showed the same *HMOX1* trend (Figure 3B). Cu did not induce the expression of *SOD1* in mock cells; however the expression of *SOD1* was significantly increased in TFEB-transfected HEK-293 cells treated with Cu (1.51 ± 0.12 -fold increase, $P < 0.05$). The effect of Cu was concentration-dependent as treating the cells for 48 h with increasing concentrations of CuCl_2 (0, 1, 10 and 100 μM) revealed that *HMOX1* expression gradually increased with Cu (Figure 3C). These data suggest that TFEB-overexpressing cells have an increased response to ROS induced by prolonged exposure to high levels of Cu.

What is the nature of the TFEB-dependent component of the Cu effect on *HMOX1*? Figure 3(D) shows that exposure to 100 mM sucrose for 48 h significantly increases *HMOX1* expression in TFEB, but not mock-transfected cells (5.95 ± 0.65 -fold increase; three independent experiment; t test $P < 0.01$ compared with untreated or treated mock-transfected cells, in which *HMOX1* mRNA showed 1.56 ± 0.30 -fold increase; independent experiments; t test $P = 0.083$). These data indicate that either *HMOX1* expression is directly controlled by TFEB or that sucrose-induced lysosomal deficits raise ROS. Analysis of *HMOX1* promoter revealed the presence of a consensus CLEAR network sequence near the *HMOX1* promoter (result not shown). The consensus sequence GTGCACTG is found at position –11 from the transcription initiation site for *HMOX1*. Furthermore, *HMOX1* is listed among the genes regulated by TFEB in the earlier studies that identified TFEB as a master regulator of lysosomal function [33,36].

To gauge the contribution of ROS-dependent and CLEAR-dependent components of *HMOX1* response to Cu, we analysed this response in the presence of the antioxidant glutathione (GSH) along with 100 μM CuCl_2 for 8 h. The short exposure to Cu was to eliminate the possible compensatory effects of expression of genes whose products play an antioxidant role. Figure 3(E) shows that co-incubation with GSH almost completely abolished the effect of Cu on *HMOX1* expression, suggesting that after 8 h of Cu exposure the expression of *HMOX1* is mainly activated by ROS and that at least at this time point, TFEB does not directly activate *HMOX1*. To test whether or not ROS are required for the activation of *HMOX1* expression after long Cu exposure, we pre-treated TFEB transfected cells with 100 μM CuCl_2 for 40 h, followed by co-incubation with GSH and Cu for an additional 8 h. At this time point, GSH was able to significantly reduce the levels of *HMOX1* expression induced by Cu, but it did not completely abolish the effect of Cu as cells treated with both Cu and GSH showed significantly higher levels of *HMOX1* compared with untreated cells (Figure 3E). These data suggest that after long Cu exposure, TFEB may regulate *HMOX1* expression in a ROS-independent manner. Since this time-frame is compatible with the time required for the TFEB-dependent activation of CLEAR network genes by Cu, we conclude that within the longer time-frame of exposure, TFEB has a direct effect on the expression of *HMOX1*, a gene whose product is an antioxidant.

ROS are damaging to several key cellular components, including mitochondria. With this in mind, we analysed the effect of Cu on mitochondrial membrane potential, as a readout of overall cellular health. Cells were treated with 1, 10 or 100 μM CuCl_2 or left untreated and analysed in a fluorometer, using the mitochondrial membrane potential sensitive dye JC-1. In the presence of mitochondrial membrane potential, JC-1 accumulates in the mitochondria resulting in a shift of fluorescence emission from green to red. Loss of mitochondrial membrane potential is detected as a decrease in the red to green ratio of JC-1 [67,68]. Interestingly, basal mitochondrial membrane potential was significantly increased (by $44.00 \pm 9.62\%$, $n=4$; Figure 4A) in TFEB-transfected cells compared with cells transfected with an empty vector, indicative of healthier mitochondria in TFEB-overexpressing cells under the resting conditions. This hyperpolarization of mitochondria can be attributed to a faster turnover of damaged mitochondria through TFEB-induced autophagy. This is consistent with the role of autophagy and lysosomes in maintaining healthy mitochondria [69,70]. CCCP, an uncoupler of the mitochondrial electron transport chain, was used as a control; it significantly decreased the mitochondrial membrane potential in both mock and TFEB-treated cells (Figure 4A).

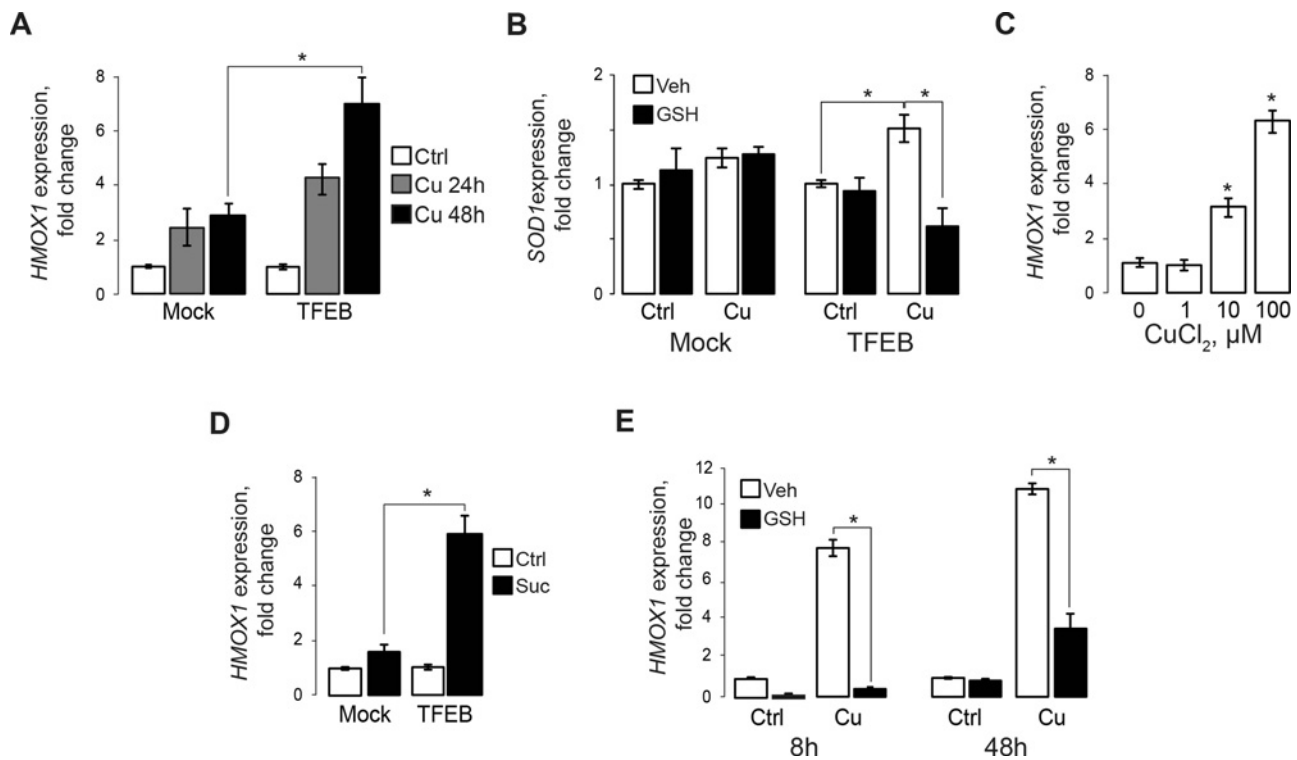


Figure 3 Cu increases the expression of *HMOX1* in HEK-293 cells

(A) qPCR analysis of *HMOX1* expression of mock or TFEB HEK-293 cells exposed to 100 μM CuCl_2 for 24 or 48 h. (B) Cu induces the expression of *SOD1* mRNA in TFEB cells, but not mock cells, treated with 100 μM CuCl_2 for 8 h in the presence or absence of 2 mM GSH. (C) qPCR analysis showing that *HMOX1* expression depends on CuCl_2 concentration (0, 1, 10, 100 μM CuCl_2) in TFEB-transfected cells. (D) Expression of *HMOX1* mRNA is increased by sucrose in TFEB-transfected cells shown by qPCR analysis. Values represented as mean \pm S.E.M. of three independent experiments; statistical significance was calculated using a two-tailed, unpaired *t* test with $P < 0.05$ considered significant (*). (A–C). (E) *HMOX1* expression in TFEB-transfected cells upon treatment with 100 μM CuCl_2 for 8 or 48 h with or without 2 mM GSH for 8 h. Values represented as mean \pm S.E.M. of two independent experiments; statistical significance was calculated using a two-tailed, unpaired *t* test with $P < 0.05$ considered significant (*).

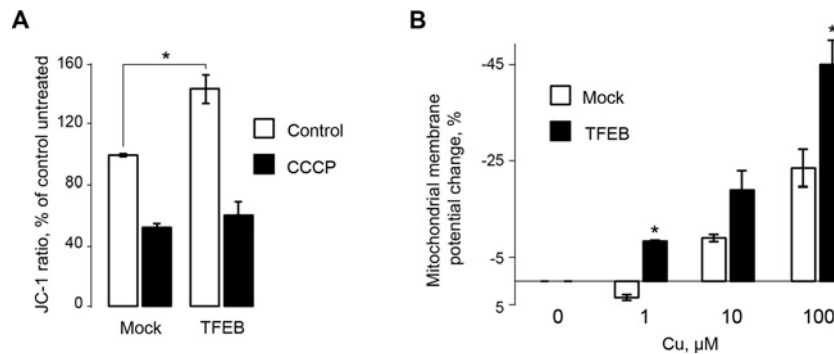


Figure 4 Cu decreases mitochondrial membrane potential

TFEB and mock HEK-293 cells were treated with 0, 1, 10, 100 μM CuCl_2 for 48 h and mitochondrial membrane potential was assessed using JC-1 dye. (A) Red/green JC-1 ratio shows that TFEB-transfected cells have higher mitochondrial membrane potential than mock-transfected cells. (B) Reduction in mitochondrial membrane potential is dependent on CuCl_2 concentration in both mock and TFEB-transfected cells. Plots represent the difference between JC-1 ratio of no Cu and Cu for mock and TFEB-cells. (*) Represents statistically significant difference (a two-tailed, unpaired *t* test with $P < 0.05$) relative to the values recorded in similarly treated mock-transfected cells.

Cu caused depolarization of mitochondrial membrane in a dose-dependent manner in both mock and TFEB-transfected cells. Consistent with the higher levels of oxidative stress in TFB-overexpressing cells exposed to Cu, the hyperpolarization observed in TFEB cells was not sufficient to prevent the loss of membrane potential caused by Cu. In fact, we observed that the decrease in membrane potential was much more dramatic in TFEB-overexpressing cells than in cells transfected with an empty vector (Figure 4B). At 1 μM CuCl_2 , the mitochondrial membrane

potential of mock-transfected cells remained unaffected whereas it was decreased by $8.36 \pm 1.59\%$ in TFEB cells ($n=3$, $P < 0.01$). Mitochondrial membrane potential of cells exposed to 10 μM CuCl_2 was decreased by $9.03 \pm 0.83\%$ in mock and $19.02 \pm 3.79\%$ ($n=3$, $P = 0.06$) in TFEB cells respectively. The highest loss of membrane potential was observed when cells were treated with 100 μM CuCl_2 and the drop in membrane potential was significantly higher in TFEB cells than in mock cells ($45.11 \pm 5.03\%$ compared with $23.48 \pm 3.89\%$ decrease

in TFEB and mock cells respectively; $P < 0.05$). These data suggested that during prolonged exposure to high levels of Cu, in HEK-293 cells, TFEB does not protect against Cu toxicity; in fact, TFEB overexpression seems to increase the toxic effects of prolonged Cu exposure in these cells.

The data described above show that Cu activates recombinant TFEB and such activation has a profound effect on the lysosomal status and on oxidative stress. This is consistent with the magnified effect of Cu exposure on oxidative stress in TFEB-overexpressing cells. Similar to the recently published data on increased cancer drug sequestration and retention in the lysosomes of TFEB overexpressing cells [44], we propose that lysosomal stress due to Cu exposure activates overexpressed TFEB and lysosomal biogenesis, increasing Cu retention in the lysosomes and, with it, ROS and oxidative stress. This is critically important for the value of TFEB up-regulation and stimulation as a therapy against oxidative stress and metal toxicity, factors involved in a range of conditions including stroke and several neurodegenerative diseases [4,6,8,53–65].

TFEB, oxidative stress and lysosomal exocytosis

TFEB was shown to have a therapeutic effect for several diseases [37,41–43], ostensibly by enhancing cellular clearance of toxic compounds. One of the mechanisms of such clearance was proposed to be enhancing lysosomal exocytosis [71,72]. The recently published data [27], including our analysis of Zn and Cu handling [20,28] strongly indicates a key role of lysosomal exocytosis in clearance of transition metals. Why was recombinant TFEB toxic when HEK-293 cells were exposed to Cu? We proposed that lysosomal exocytosis is a rate-limiting step in the TFEB-dependent lysosomal clearance process, and, in TFEB-overexpressing HEK-293 cells, increased sequestration and retention of Cu in the lysosomes is not effectively countered by lysosomal exocytosis, leading to enhanced oxidative stress. A corollary hypothesis is that TFEB will have more cytoprotective effects in cells with high rates of lysosomal exocytosis. Not aware of a way to specifically up-regulate lysosomal exocytosis by pharmacological or genetic means, we sought to test our model using cells with higher lysosomal exocytosis rates. HEK-293 cells do not appear to have a robust lysosomal exocytosis process as indicated by exocytosis of the lysosomal enzyme β -hexosaminidase (β -Hex, Figure 5A) [73]. By contrast, HeLa cells showed robust β -Hex and transition metal exocytosis [20,28] and these cells were chosen to supplement the data obtained with HEK-293 cells.

Figure 5(B) shows that when HeLa cells were exposed to 1–100 μ M Cu for a period of 1–16 h, mock-transfected cells displayed increased *HMOX1* mRNA levels, indicative of increased oxidative stress. Mock-transfected cells showed a measureable increase in *HMOX1* mRNA at 1 μ M Cu after 1-h exposure (1.54 ± 0.09 -fold increase, $P < 0.05$, $n=3$). Under these conditions, such an increase was not pronounced in TFEB-transfected HeLa cells. Sixteen-hour long exposure to 100 μ M Cu induced a significant increase in *HMOX1* mRNA in mock-transfected cells: 10.30 ± 0.94 -fold increase ($P < 0.05$, $n=3$), whereas such an increase averaged only 5.53 ± 0.47 -fold in TFEB-transfected cells. These data suggest that in HeLa cells TFEB has a cytoprotective effect at short exposure and low levels of Cu.

Interestingly, the trend did not persist at longer exposure times as 24-h long exposure to Cu caused the same change in *HMOX1* expression in mock- as in TFEB-expressing cells (Figure 5C). Lysosomal exocytosis is regulated by ionic events including Ca^{2+} -dependent SNARE (SNAP (soluble NSF attachment protein)

receptor) interaction [73] and it is possible that Cu interferes with some aspect of the SNARE function. The importance of lysosomal exocytosis for Cu detoxification is illustrated in Figure 5(D); in HeLa cells, the response of *HMOX1* to Cu is accentuated by the siRNA-dependent knockdown of the lysosomal-plasma membrane SNARE VAMP7 (vesicle-associated membrane protein 7). Figure 5(E) shows that prolonged exposure to high concentrations of Cu inhibits β -Hex exocytosis. In accordance with the previous evidence, TFEB overexpression stimulates β -Hex exocytosis, but it does not eliminate the inhibitory effect of high Cu exposure (Figure 5E). Based on these results, we propose that TFEB increases the lysosomal capacity for exocytosis and with it, Cu detoxification. However, under conditions of chronic exposure to high Cu levels, the TFEB effect is toxic, ostensibly due to an increase in the lysosomal Cu absorption capacity, a but decrease in their exocytosis. This is a novel aspect of Cu toxicity.

DISCUSSION

In the course of the present studies, we have shown that exposure to transition metals activates recombinant overexpressed TFEB. Cu exposure was associated with TFEB dephosphorylation, resulting in activation of TFEB-dependent transcription. We have also shown that TFEB regulates the expression of *HMOX1*, a gene involved in the response to oxidative stress. Although *HMOX1* has been previously identified as being part of the network of TFEB-regulated genes, this is the first time that *HMOX1* expression and oxidative stress have been directly linked to TFEB activity. Additionally, our data contribute to a better understanding of the therapeutic potential of TFEB activation or overexpression by identifying some of the margins for its effects.

We show that recombinant TFEB protects against Cu toxicity at moderate levels of Cu exposure, but it is more toxic at high levels of exposure; in fact, in HEK-293 cells, TFEB overexpression aggravated the Cu-induced loss of membrane potential despite increasing mitochondrial membrane potential under basal conditions (Figure 4). It does not seem likely that such an effect includes cytoplasmic Cu, as we failed to detect measureable differences in cytoplasmic Cu between mock- and TFEB-transfected cells using the protein levels of the Cu chaperone to superoxide dismutase, CCS [74,75]. CCS delivers Cu to superoxide dismutase and it has been shown that in the presence of high levels of Cu the proteasome-dependent degradation of CCS is induced [76], as Cu is more available to superoxide dismutase. Supplementary Figure S4 shows that overexpression of TFEB did not affect the reduction in CCS levels after 24 h exposure to 100 μ M CuCl_2 , as both mock- and TFEB-overexpressing HEK-293 cells presented a reduction of $\sim 60\%$ in CCS levels. These data suggest that TFEB overexpression does not cause a major retention of Cu in the cytoplasm.

The toxic effect of TFEB overexpression in HEK-293 cells is probably due to their lack of efficient lysosomal exocytosis (Figure 5A). In contrast, cells with robust lysosomal exocytosis, such as HeLa cells, are more likely to manifest the cytoprotective function of TFEB. Although transition metals are effectively secreted with lysosomal exocytosis [20,27], it is possible that Cu interferes with that exocytosis mechanism in several ways. Others and we have recently shown that brief (1–8 h) exposure to Cu activates lysosomal exocytosis [27,28]. However, prolonged exposure to Cu seems to suppress lysosomal exocytosis in HeLa cells as shown in Figure 5(E). It is possible that short and long exposures to Cu have different effects on various components of the lysosomal exocytosis machinery.

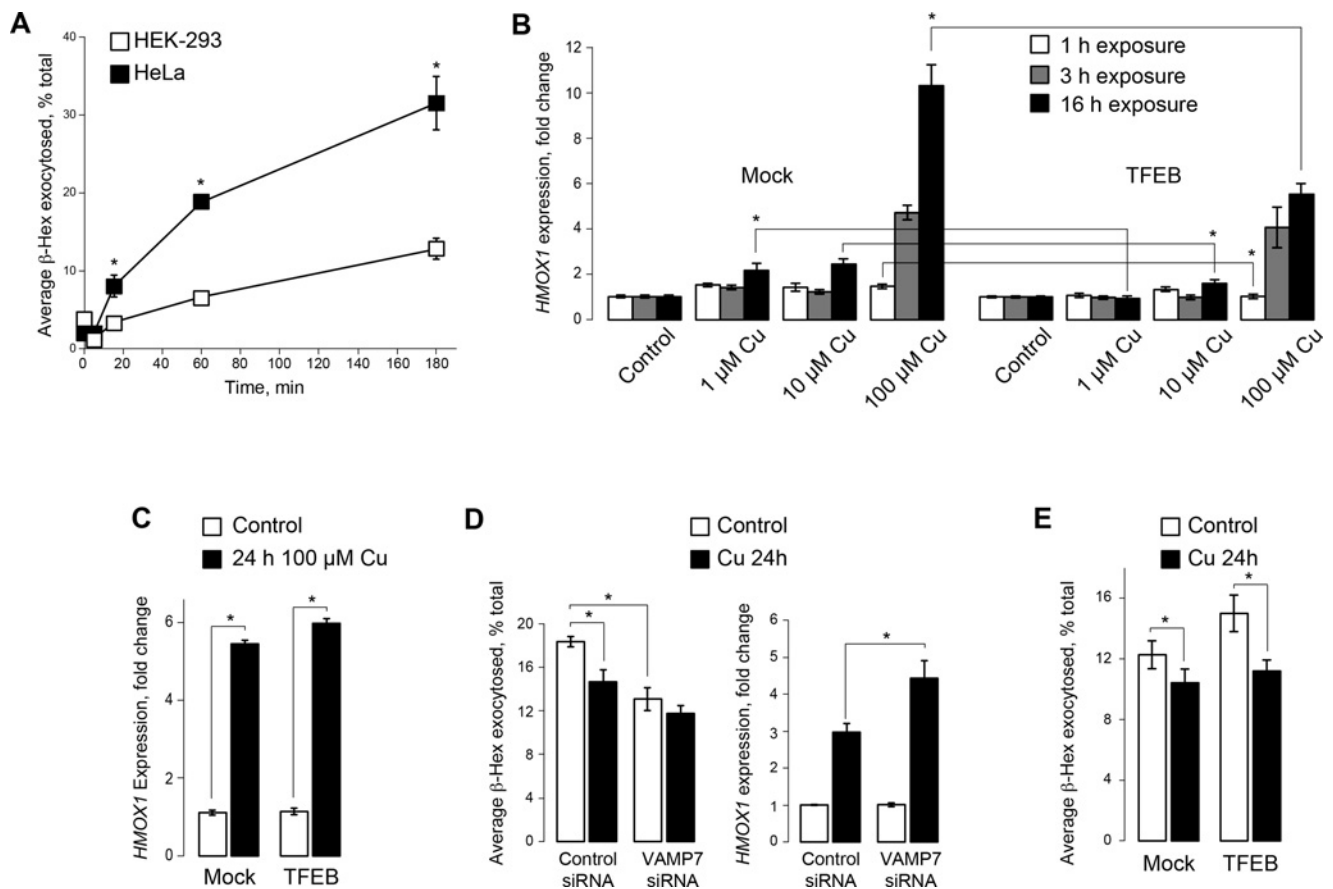


Figure 5 TFEB decreases oxidative stress induced by moderate Cu exposure in HeLa cells

(A) Time course of β -Hex exocytosis assay in HEK-293 and HeLa cells. β -Hex levels in the medium were measured at 0, 5, 15, 60 and 180 min. HeLa cells exhibit a higher rate of lysosomal exocytosis than HEK-293 cells. (B) qPCR analysis of *HMOX1* expression in mock- or TFEB-transfected HeLa cells exposed to 1, 10 and 100 μ M CuCl_2 for 1, 3 and 16 h. Data were normalized to the corresponding untreated controls, which were taken as 1. (C) The same experiments performed at 24-h time point, with 100 μ M Cu. (D) β -Hex exocytosis (left panel) and *HMOX1* expression (right panel) in HeLa cells treated with Cu as a function lysosomal exocytosis, which was suppressed using VAMP7 siRNA. β -Hex levels in the medium were measured after 1 h of exocytosis. (E) Lysosomal exocytosis (β -Hex exocytosis) in mock- and TFEB-transfected HeLa cells treated with Cu. Values represented as mean \pm S.E.M. of three independent experiments; statistical significance was calculated using a two-tailed, unpaired *t* test with $P < 0.05$ (*) considered significant.

We have also shown that Cu exposure induces dephosphorylation of exogenous TFEB and subsequent nuclear translocation, resulting in increased expression of lysosomal genes (Figure 1). The mechanism by which Cu activates TFEB remains to be elucidated. A likely mechanism of TFEB activation by Cu is the lysosomal deficits in Cu-treated cells. mTORC1 activity requires functional V-type ATPase [77]. Inhibition of the ATPase by Cu should cause mTORC1 inhibition and TFEB activation. Furthermore, it has been shown that changes in lysosomal positioning can affect mTORC1 activity [78]. In fact, Korolchuk et al. [78] showed that clustering of lysosomes due to disrupted transport leads to a reduced mTORC1 activity. Since TFEB is activated when mTORC1 activity is inhibited, defects in lysosomal transport could induce the activation of TFEB. Therefore, the aggregation of lysosomes could be a consequence of disrupted lysosomal transport in response to Cu, inducing the inactivation of mTORC1. In this scenario, an increased number of lysosomes will result in more lysosomal aggregates, in agreement with the increased number of aggregates observed in TFEB-overexpressing cells treated with Cu (Figure 2C). An effect of Cu (or Cu-induced ROS) on lysosomal traffic may account for the reported effects of Cu on lysosomal exocytosis.

Interestingly, in HEK-293 cells TFEB overexpression caused an increase in mitochondrial membrane potential (Figure 4). It is possible that this observation is due to up-regulation of mitophagy of damaged mitochondria as a consequence of TFEB overexpression. Additionally, TFEB overexpression could increase mitochondrial biogenesis, as has been recently shown [79,80], resulting in a higher mitochondrial membrane potential due to an increased number of mitochondria. Another possibility is that TFEB directly regulates mitochondrial genes associated with membrane potential; although there is no evidence showing direct regulation of such genes by TFEB, genes involved in the tricarboxylic acid (TCA) cycle and mitochondrial oxidative phosphorylation have been listed as direct targets of TFEB [33]. It is not surprising that TFEB can regulate biogenesis and gene expression of organelles other than the lysosome; in fact, TFEB3, a TFEB relative, has been shown to regulate the expression of genes involved in the Golgi apparatus function and stress response [81]. All this evidence supports our idea that TFEB can regulate different cellular processes, as discussed below.

In addition to these observations, our data show that TFEB may be involved in the response to oxidative stress. The earlier studies describing the gene network regulated by TFEB have identified several genes that contain a TFEB-binding sequence or CLEAR

element and they are involved in different cellular pathways; however, studies have been focused on the genes that regulate lysosomal-associated processes. Among the genes that are not directly related to the lysosome is *HMOX1*. It should be noted that *HMOX1* and other genes involved in oxidative stress response, such as *GPX1* (glutathione peroxidase 1) and *GSTO1* (*GST* ω 1), are found in the original set of genes identified as TFEB-dependent [33,36]. The fact that *HMOX1* promoter region appears to contain a full CLEAR sequence suggests an exciting possibility that beyond their role in lysosomal biogenesis, TFEB may drive a broader stress response mechanism, involving antioxidant genes. Indeed, we have shown that Cu induces expression of *HMOX1* in a ROS-dependent manner; however, our data also indicate that only a fraction of *HMOX1* expression depends solely on TFEB activation. This is evidenced by the increase in *HMOX1* mRNA levels observed in TFEB overexpressing cells treated with sucrose and by the fact that GSH did not completely abolish the expression of *HMOX1* after long exposure to Cu (Figure 5E). Furthermore, the basal levels of *HMOX1* in TFEB overexpressing cells were 30% higher than in cells transfected with an empty vector (result not shown). With this in mind, we cannot rule out the possibility that TFEB controls the function of other transcription factors involved in the response to oxidative stress, such as MTF-1 and NRF2, the latest known to regulate the expression of *HMOX1* as well. The role of TFEB in the oxidative stress response is an interesting aspect that has not been explored before. Future studies should focus on the role of TFEB in oxidative stress, especially because there is increasing evidence showing the relationship between autophagy and ROS [82,83].

The expression of lysosomal genes is regulated not only by TFEB. It has recently been shown that TFE3 regulates the expression of genes involved in autophagy and is activated in response to lysosomal stress [35,39,47]. TFE3 also binds to promoter regions containing the CLEAR sequence, thus it may control the expression of TFEB-regulated genes as well. As shown in Supplementary Figure S1(C), TFE3 overexpression reversed the drop in gene expression after Cu treatment; however, the increase in gene expression in response to Cu was somewhat lower than the one observed in TFEB-transfected cells. At present, we do not know the reason for the lower magnitude of the TFE3-dependent response to Cu. Since both TFEB and TFE3 seem to receive input from the same TFE3-dependent signalling pathway, it is likely that some events or processes downstream of TFEB/TFE3 activation are responsible for these differences. Such processes may include efficacy of transcriptional activation or some other regulatory mechanisms converging on these transcription factors downstream of their activation. As shown in Figure 1 and Supplementary Figure S1, in mock-transfected cells, Cu exposure causes a loss of mRNA corresponding to several lysosomal genes. Whether or not oxidative stress is a factor in the differences between TFEB and TFE3 efficacy remains to be elucidated.

A related issue exists with the status of native TFEB/TFE3 responses in our model. TFEB overexpression has been used to study its activation and the resulting up-regulation of the lysosomal gene network in the vast majority of reports utilizing cell cultures. It is important to note that it was not only Cu that showed low activation of endogenous TFEB; accordingly, we were unable to consistently detect activation of the lysosomal gene network using native TFEB stimulated by starvation, sucrose or the TFEB activator torin 1 [84] in HEK-293, HeLa, RPE-1 or HUH-7 cells, consistent with low levels of TFEB in these cells and with previously published results [38,39,43,85,86]. In experiments in which such activation was detected, we also saw activation of lysosomal gene expression by Cu (Supplementary

Figure S5); however, the small amplitude and poor reproducibility of these responses precluded its further analysis. The reasons for these effects are unclear, but very low levels of native TFEB/TFE3 in these cells have been suggested. Their scarcity may become very important if oxidative stress does, indeed, affect stability of mRNA corresponding to the 'lysosomal' genes, resulting in the loss of mRNA as shown in Figure 1 and Supplementary Figure S1. It is possible that cultured cells are not prepared to respond to nutrient starvation or lysosomal stress because they normally grow in optimal conditions of nutrient abundance, thus they are not required to keep high basal levels of TFEB. This may make them less likely to respond to other lysosomal stressors, including Cu.

The data described in the present study suggest that Cu and Fe activate overexpressed TFEB and this activation leads to a measurable change in lysosomal status and the ability of cells to fight oxidative stress caused by transition metal exposure. We show that the full cytoprotective effect of TFEB manifests only when cells have robust lysosomal exocytosis. Indeed, TFEB overexpression seems to increase transition metal toxicity in cells with low lysosomal exocytosis rates. These data suggest that the cytoprotective function of TFEB fully manifests when lysosomal exocytosis is effective, which is not the case for all cell types. Therefore it is tempting to suggest that therapies involving TFEB activation or up-regulation should also focus on pharmacological stimulation of lysosomal exocytosis.

AUTHOR CONTRIBUTION

Karina Peña designed and executed the experiments and analyzed the data. Kirill Kiselyov designed the experiments and analyzed the data.

ACKNOWLEDGEMENT

We thank Dr Rosa Puertollano and Dr Jose Martina for the TFEB and TFE3 constructs and for help with them. We are grateful to Dr Dennis Thiele for the discussion and for CCS antibodies. We thank Sreeram Ravi for technical help.

FUNDING

This work was supported by the National Institutes of Health [grant numbers HD058577 and ES01678] to K.K.

REFERENCES

- Bleackley, M.R. and Macgillivray, R.T. (2011) Transition metal homeostasis: from yeast to human disease. *Biometals* **24**, 785–809 [CrossRef PubMed](#)
- Pankit, A.N. and Bhawe, S.A. (2002) Copper metabolic defects and liver disease: environmental aspects. *J. Gastroenterol. Hepatol* **17** Suppl 3, S403–S407 [CrossRef PubMed](#)
- Aston, N.S., Watt, N., Morton, I.E., Tanner, M.S. and Evans, G.S. (2000) Copper toxicity affects proliferation and viability of human hepatoma cells (HepG2 line). *Hum. Exp. Toxicol.* **19**, 367–376 [CrossRef PubMed](#)
- Hayashi, H., Yano, M., Fujita, Y. and Wakusawa, S. (2006) Compound overload of copper and iron in patients with Wilson's disease. *Med. Mol. Morphol* **39**, 121–126 [CrossRef PubMed](#)
- Llanos, R.M. and Mercer, J.F. (2002) The molecular basis of copper homeostasis copper-related disorders. *DNA Cell Biol* **21**, 259–270 [CrossRef PubMed](#)
- Schrag, M., Mueller, C., Oyoyo, U., Smith, M.A. and Kirsch, W.M. (2011) Iron, zinc and copper in the Alzheimer's disease brain: a quantitative meta-analysis. Some insight on the influence of citation bias on scientific opinion. *Prog. Neurobiol.* **94**, 296–306 [CrossRef PubMed](#)
- Shcherbatykh, I. and Carpenter, D.O. (2007) The role of metals in the etiology of Alzheimer's disease. *J. Alzheimers Dis.* **11**, 191–205 [PubMed](#)

- 8 Tougu, V., Tiiman, A. and Palumaa, P. (2011) Interactions of Zn(II) and Cu(II) ions with Alzheimer's amyloid-beta peptide. Metal ion binding, contribution to fibrillization and toxicity. *Metallomics* **3**, 250–261 [CrossRef PubMed](#)
- 9 Ward, R.J., Dexter, D.T. and Crichton, R.R. (2012) Chelating agents for neurodegenerative diseases. *Curr. Med. Chem* **19**, 2760–2772 [CrossRef PubMed](#)
- 10 Dexter, D.T., Carayon, A., Javoy, A.F., Agid, Y., Wells, F.R., Daniel, S.E., Lees, A.J., Jenner, P. and Marsden, C.D. (1991) Alterations in the levels of iron, ferritin and other trace metals in Parkinson's disease and other neurodegenerative diseases affecting the basal ganglia. *Brain* **114**, 1953–1975 [CrossRef PubMed](#)
- 11 Dexter, D.T., Sian, J., Rose, S., Hindmarsh, J.G., Mann, V.M., Cooper, J.M., Wells, F.R., Daniel, S.E., Lees, A.J., Schapira, A.H. et al. (1994) Indices of oxidative stress and mitochondrial function in individuals with incidental Lewy body disease. *Ann. Neurol.* **35**, 38–44 [CrossRef PubMed](#)
- 12 Mendez-Alvarez, E., Soto-Otero, R., Hermida-Ameijeiras, A., Lopez-Real, A.M. and Labandeira-Garcia, J.L. (2002) Effects of aluminum and zinc on the oxidative stress caused by 6-hydroxydopamine autoxidation: relevance for the pathogenesis of Parkinson's disease. *Biochim. Biophys. Acta* 155–168 [PubMed](#)
- 13 Riederer, P., Sofic, E., Rausch, W.D., Schmidt, B., Reynolds, G.P., Jellinger, K. and Youdim, M.B. (1989) Transition metals, ferritin, glutathione, and ascorbic acid in parkinsonian brains. *J. Neurochem.* **52**, 515–520 [CrossRef PubMed](#)
- 14 Barnham, K.J., Masters, C.L. and Bush, A.I. (2004) Neurodegenerative diseases and oxidative stress. *Nat. Rev. Drug Discov.* **3**, 205–214 [CrossRef PubMed](#)
- 15 Halliwell, B. and Gutteridge, J.M.C. (1984) Oxygen toxicity, oxygen radicals, transition metals and disease. *Biochem. J.* **219**, 1–14 [PubMed](#)
- 16 Hegde, M.L., Hegde, P.M., Rao, K.S. and Mitra, S. (2011) Oxidative genome damage and its repair in neurodegenerative diseases: function of transition metals as a double-edged sword. *J. Alzheimers Dis.* **24** Suppl 2, 183–198 [PubMed](#)
- 17 Hill, G.M. and Link, J.E. (2009) Transporters in the absorption and utilization of zinc and copper. *J. Anim. Sci.* **87**, E85–E89 [CrossRef PubMed](#)
- 18 Morgan, E.H. and Oates, P.S. (2002) Mechanisms and regulation of intestinal iron absorption. *Blood Cells Mol. Dis.* **29**, 384–399 [CrossRef PubMed](#)
- 19 Bouron, A. and Oberwinkler, J. (2014) Contribution of calcium-conducting channels to the transport of zinc ions. *Pflügers Arch* **466**, 381–387 [CrossRef PubMed](#)
- 20 Kucic, I., Kelleher, S.L. and Kiselyov, K. (2014) Zn²⁺ efflux through lysosomal exocytosis prevents Zn²⁺-induced toxicity. *J. Cell Sci.* **127**, 3094–3103 [CrossRef PubMed](#)
- 21 Kucic, I., Lee, J.K., Coblenz, J., Kelleher, S.L. and Kiselyov, K. (2013) Zinc-dependent lysosomal enlargement in TRPML1-deficient cells involves MTF-1 transcription factor and ZnT4 (Slc30a4) transporter. *Biochem. J.* **451**, 155–163 [CrossRef PubMed](#)
- 22 Lopez, V. and Kelleher, S.L. (2009) Zinc transporter-2 (ZnT2) variants are localized to distinct subcellular compartments and functionally transport zinc. *Biochem. J.* **422**, 43–52 [CrossRef PubMed](#)
- 23 Lopez, V., Foolad, F. and Kelleher, S.L. (2011) ZnT2-overexpression represses the cytotoxic effects of zinc hyper-accumulation in malignant metallothionein-null T47D breast tumor cells. *Cancer Lett* **304**, 41–51 [CrossRef PubMed](#)
- 24 Seo, Y.A. and Kelleher, S.L. (2010) Functional analysis of two single nucleotide polymorphisms in SLC30A2 (ZnT2): implications for mammary gland function and breast disease in women. *Physiol. Genomics* **42A**, 219–227 [CrossRef PubMed](#)
- 25 Harada, M., Kawaguchi, T., Kumemura, H., Terada, K., Ninomiya, H., Taniguchi, E., Hanada, S., Baba, S., Maeyama, M., Koga, H. et al. (2005) The Wilson disease protein ATP7B resides in the late endosomes with Rab7 and the Niemann-Pick C1 protein. *Am. J. Pathol.* **166**, 499–510 [CrossRef PubMed](#)
- 26 Chapel, A., Kieffer-Jaquinod, S., Sagne, C., Verdon, Q., Ivaldi, C., Mellal, M., Thirion, J., Jadot, M., Bruley, C., Garin, J. et al. (2013) An extended proteome map of the lysosomal membrane reveals novel potential transporters. *Mol. Cell. Proteomics* **12**, 1572–1588 [CrossRef PubMed](#)
- 27 Polishchuk, E.V., Concilli, M., Iacobacci, S., Chesi, G., Pastore, N., Piccolo, P., Paladino, S., Baldantoni, D., van, I.S.C., Chan, J. et al. (2014) Wilson disease protein ATP7B utilizes lysosomal exocytosis to maintain copper homeostasis. *Dev. Cell* **29**, 686–700 [CrossRef PubMed](#)
- 28 Pena, K., Coblenz, J. and Kiselyov, K. (2015) Brief exposure to copper activates lysosomal exocytosis. *Cell Calcium* **57**, 257–262 [CrossRef PubMed](#)
- 29 Valerio, L.G. (2007) Mammalian iron metabolism. *Toxicol. Mech. Methods* **17**, 497–517 [CrossRef PubMed](#)
- 30 Coblenz, J., St Croix, C. and Kiselyov, K. (2014) Loss of TRPML1 promotes production of reactive oxygen species: is oxidative damage a factor in mucopolidosis type IV? *Biochem. J.* **457**, 361–368 [CrossRef PubMed](#)
- 31 Eichelsdoerfer, J.L., Evans, J.A., Slaugenhaupt, S.A. and Cuajungco, M.P. (2010) Zinc dyshomeostasis is linked with the loss of mucopolidosis IV-associated TRPML1 ion channel. *J. Biol. Chem.* **285**, 34304–34308 [CrossRef PubMed](#)
- 32 Dong, X., Cheng, X., Mills, E., Delling, M., Wang, F., Kurz, T. and Xu, H. (2008) The type IV mucopolidosis-associated protein TRPML1 is an endolysosomal iron release channel. *Nature* **455**, 992–996 [CrossRef PubMed](#)
- 33 Sardiello, M., Palmieri, M., di Ronza, A., Medina, D.L., Valenza, M., Gennarino, V.A., Di Malta, C., Donaudy, F., Embrione, V., Polishchuk, R.S. et al. (2009) A gene network regulating lysosomal biogenesis and function. *Science* **325**, 473–477 [PubMed](#)
- 34 Settembre, C., Di Malta, C., Polito, V.A., Garcia Arencibia, M., Vetriani, F., Erdin, S., Erdin, S.U., Huynh, T., Medina, D., Colella, P. et al. (2011) TFEB links autophagy to lysosomal biogenesis. *Science* **332**, 1429–1433 [CrossRef PubMed](#)
- 35 Martina, J.A., Diab, H.I., Lishu, L., Jeong, A.L., Patange, S., Raben, N. and Puertollano, R. (2014) The nutrient-responsive transcription factor TFEB promotes autophagy, lysosomal biogenesis, and clearance of cellular debris. *Sci. Signal.* **7**, ra9 [CrossRef PubMed](#)
- 36 Palmieri, M., Impey, S., Kang, H., di Ronza, A., Pelz, C., Sardiello, M. and Ballabio, A. (2011) Characterization of the CLEAR network reveals an integrated control of cellular clearance pathways. *Hum. Mol. Genet.* **20**, 3852–3866 [CrossRef PubMed](#)
- 37 Medina, D.L., Fraldi, A., Bouche, V., Annunziata, F., Mansueti, G., Spampinato, C., Puri, C., Pignata, A., Martina, J.A., Sardiello, M. et al. (2011) Transcriptional activation of lysosomal exocytosis promotes cellular clearance. *Dev. Cell.* **21**, 421–430 [CrossRef PubMed](#)
- 38 Martina, J.A., Chen, Y., Gucek, M. and Puertollano, R. (2012) MTORC1 functions as a transcriptional regulator of autophagy by preventing nuclear transport of TFEB. *Autophagy* **8**, 903–914 [CrossRef PubMed](#)
- 39 Rocznik-Ferguson, A., Petit, C.S., Froehlich, F., Qian, S., Ky, J., Angarola, B., Walther, T.C. and Ferguson, S.M. (2012) The transcription factor TFEB links mTORC1 signaling to transcriptional control of lysosome homeostasis. *Sci. Signal.* **5**, ra2 [CrossRef PubMed](#)
- 40 Settembre, C., Zoncu, R., Medina, D.L., Vetriani, F., Erdin, S., Huynh, T., Ferron, M., Karsenty, G., Vellard, M.C., Facchinetti, V. et al. (2012) A lysosome-to-nucleus signalling mechanism senses and regulates the lysosome via mTOR and TFEB. *EMBO J* **31**, 1095–1108 [CrossRef PubMed](#)
- 41 La Spada, A.R. (2012) PPARGC1A/PGC-1alpha, TFEB and enhanced proteostasis in Huntington disease: Defining regulatory linkages between energy production and protein-organelle quality control. *Autophagy* **8**, 1845–1847 [CrossRef PubMed](#)
- 42 Decressac, M., Mattsson, B., Weikop, P., Lundblad, M., Jakobsson, J. and Bjorklund, A. (2013) TFEB-mediated autophagy rescues midbrain dopamine neurons from alpha-synuclein toxicity. *Proc. Natl. Acad. Sci. U.S.A.* **110**, E1817–E1826 [CrossRef PubMed](#)
- 43 Pastore, N., Blomenkamp, K., Annunziata, F., Piccolo, P., Mithbaokar, P., Maria Sepe, R., Vetriani, F., Palmer, D., Ng, P., Polishchuk, E. et al. (2013) Gene transfer of master autophagy regulator TFEB results in clearance of toxic protein and correction of hepatic disease in alpha-1-anti-trypsin deficiency. *EMBO Mol. Med.* **5**, 397–412 [CrossRef PubMed](#)
- 44 Zhitomirsky, B. and Assaraf, Y.G. (2015) Lysosomal sequestration of hydrophobic weak base chemotherapeutics triggers lysosomal biogenesis and lysosome-dependent cancer multidrug resistance. *Oncotarget* **6**, 1143–1156 [PubMed](#)
- 45 Pourahmad, J., Ross, S. and O'Brien, P.J. (2001) Lysosomal involvement in hepatocyte cytotoxicity induced by Cu(2+) but not Cd(2+). *Free Radic. Biol. Med.* **30**, 89–97 [CrossRef PubMed](#)
- 46 Singh, R.P., Kumar, S., Nada, R. and Prasad, R. (2006) Evaluation of copper toxicity in isolated human peripheral blood mononuclear cells and its attenuation by zinc: *ex vivo*. *Mol. Cell Biochem* **282**, 13–21 [CrossRef PubMed](#)
- 47 Martina, J.A., Diab, H.I., Li, H. and Puertollano, R. (2014) Novel roles for the MiTF/TFE family of transcription factors in organelle biogenesis, nutrient sensing, and energy homeostasis. *Cell. Mol. Life Sci.* **71**, 2483–2497 [CrossRef PubMed](#)
- 48 Brunk, U.T., Jones, C.B. and Sohal, R.S. (1992) A novel hypothesis of lipofuscinogenesis and cellular aging based on interactions between oxidative stress and autophagocytosis. *Mutat. Res.* **275**, 395–403 [CrossRef PubMed](#)
- 49 Colletti, G.A., Miedel, M.T., Quinn, J., Andharia, N., Weisz, O.A. and Kiselyov, K. (2012) Loss of lysosomal ion channel transient receptor potential channel mucolipin-1 (TRPML1) leads to cathepsin B-dependent apoptosis. *J. Biol. Chem.* **287**, 8082–8091 [CrossRef PubMed](#)
- 50 Dusek, P., Jankovic, J. and Le, W. (2012) Iron dysregulation in movement disorders. *Neurobiol. Dis.* **46**, 1–18 [CrossRef PubMed](#)
- 51 Kurz, T., Terman, A., Gustafsson, B. and Brunk, U.T. (2008) Lysosomes in iron metabolism, ageing and apoptosis. *Histochem. Cell. Biol.* **129**, 389–406 [CrossRef PubMed](#)
- 52 Dong, X.P., Cheng, X., Mills, E., Delling, M., Wang, F., Kurz, T. and Xu, H. (2008) The type IV mucopolidosis-associated protein TRPML1 is an endolysosomal iron release channel. *Nature* **455**, 992–996 [CrossRef PubMed](#)
- 53 Roberts, B.R., Ryan, T.M., Bush, A.I., Masters, C.L. and Duce, J.A. (2012) The role of metallobiology and amyloid-beta peptides in Alzheimer's disease. *J. Neurochem* **120** Suppl 1, 149–166 [CrossRef PubMed](#)
- 54 Shuttleworth, C.W. and Weiss, J.H. (2011) Zinc: new clues to diverse roles in brain ischemia. *Trends Pharmacol. Sci.* **32**, 480–486 [CrossRef PubMed](#)
- 55 Sensi, S.L., Paoletti, P., Koh, J.Y., Aizenman, E., Bush, A.I. and Hershfinkel, M. (2011) The neurophysiology and pathology of brain zinc. *J. Neurosci.* **31**, 16076–16085 [CrossRef PubMed](#)

- 56 Galasso, S.L. and Dyck, R.H. (2007) The role of zinc in cerebral ischemia. *Mol. Med.* **13**, 380–387 [CrossRef PubMed](#)
- 57 Sheline, C.T., Zhu, J., Zhang, W., Shi, C. and Cai, A.L. (2013) Mitochondrial inhibitor models of Huntington's disease and Parkinson's disease induce zinc accumulation and are attenuated by inhibition of zinc neurotoxicity *in vitro* or *in vivo*. *Neurodegener. Dis* **11**, 49–58 [CrossRef PubMed](#)
- 58 Brewer, G.J. (2010) Risks of copper and iron toxicity during aging in humans. *Chem. Res. Toxicol.* **23**, 319–326 [CrossRef PubMed](#)
- 59 Jansen, J., Karges, W. and Rink, L. (2009) Zinc and diabetes—clinical links and molecular mechanisms. *J. Nutr. Biochem.* **20**, 399–417 [CrossRef PubMed](#)
- 60 Hordyjewska, A., Popiolek, L. and Kocot, J. (2014) The many “faces” of copper in medicine and treatment. *Biomaterials* **27**, 611–621 [CrossRef PubMed](#)
- 61 Wijmenga, C. and Klomp, L.W. (2004) Molecular regulation of copper excretion in the liver. *Proc. Nutr. Soc.* **63**, 31–39 [CrossRef PubMed](#)
- 62 Festa, R.A. and Thiele, D.J. (2011) Copper: an essential metal in biology. *Curr. Biol.* **21**, R877–883 [CrossRef PubMed](#)
- 63 Graper, M.L., Huster, D., Kaler, S.G., Lutsenko, S., Schilsky, M.L. and Thiele, D.J. (2014) Introduction to human disorders of copper metabolism. *Ann. N.Y. Acad. Sci.* **1314**, v–vi [CrossRef PubMed](#)
- 64 Hare, D., Ayton, S., Bush, A. and Lei, P. (2013) A delicate balance: Iron metabolism and diseases of the brain. *Front. Aging Neurosci.* **5**, 34 [CrossRef PubMed](#)
- 65 Zheng, Z., Lee, J.E. and Yenari, M.A. (2003) Stroke: molecular mechanisms and potential targets for treatment. *Curr. Mol. Med.* **3**, 361–372 [CrossRef PubMed](#)
- 66 Yoo, H.Y., Chang, M.S. and Rho, H.M. (1999) Heavy metal-mediated activation of the rat Cu/Zn superoxide dismutase gene via a metal-responsive element. *Mol. Gen. Genet.* **262**, 310–313 [CrossRef PubMed](#)
- 67 Cheng, W.Y., Tong, H., Miller, E.W., Chang, C.J., Remington, J., Zucker, R.M., Bromberg, P.A., Samet, J.M. and Hofer, T.P. (2010) An integrated imaging approach to the study of oxidative stress generation by mitochondrial dysfunction in living cells. *Environ. Health Perspect.* **118**, 902–908 [CrossRef PubMed](#)
- 68 White, R.J. and Reynolds, I.J. (1996) Mitochondrial depolarization in glutamate-stimulated neurons: an early signal specific to excitotoxin exposure. *J. Neurosci.* **16**, 5688–5697 [PubMed](#)
- 69 Kiselyov, K., Jennigs, Jr, J.J., Rbaibi, Y. and Chu, C.T. (2007) Autophagy, mitochondria and cell death in lysosomal storage diseases. *Autophagy* **3**, 259–262 [CrossRef PubMed](#)
- 70 Ventruti, A. and Cuervo, A.M. (2007) Autophagy and neurodegeneration. *Curr. Neurol. Neurosci. Rep.* **7**, 443–451 [CrossRef PubMed](#)
- 71 Spanpanato, C., Feeney, E., Li, L., Cardone, M., Lim, J.A., Annunziata, F., Zare, H., Polishchuk, R., Puertollano, R., Parenti, G. et al. (2013) Transcription factor EB (TFEB) is a new therapeutic target for Pompe disease. *EMBO Mol. Med.* **5**, 691–706 [CrossRef PubMed](#)
- 72 Feeney, E.J., Spanpanato, C., Puertollano, R., Ballabio, A., Parenti, G. and Raben, N. (2013) What else is in store for autophagy? Exocytosis of autolysosomes as a mechanism of TFEB-mediated cellular clearance in Pompe disease. *Autophagy* **9**, 1117–1118 [CrossRef PubMed](#)
- 73 Rao, S.K., Huynh, C., Proux-Gillardeaux, V., Galli, T. and Andrews, N.W. (2004) Identification of SNAREs involved in synaptotagmin VII-regulated lysosomal exocytosis. *J. Biol. Chem.* **279**, 20471–20479 [CrossRef PubMed](#)
- 74 Robinson, N.J. and Winge, D.R. (2010) Copper metallochaperones. *Annu. Rev. Biochem.* **79**, 537–562 [CrossRef PubMed](#)
- 75 Harris, E.D. (2000) Cellular copper transport and metabolism. *Annu. Rev. Nutr.* **20**, 291–310 [CrossRef PubMed](#)
- 76 Caruano-Yzermans, A.L., Bartnikas, T.B. and Gitlin, J.D. (2006) Mechanisms of the copper-dependent turnover of the copper chaperone for superoxide dismutase. *J. Biol. Chem.* **281**, 13581–13587 [CrossRef PubMed](#)
- 77 Zoncu, R., Bar-Peled, L., Efeyan, A., Wang, S., Sancak, Y. and Sabatini, D.M. (2011) mTORC1 senses lysosomal amino acids through an inside-out mechanism that requires the vacuolar H(+) -ATPase. *Science* **334**, 678–683 [CrossRef PubMed](#)
- 78 Korolchuk, V.I., Saiki, S., Lichtenberg, M., Siddiqi, F.H., Roberts, E.A., Imarisio, S., Jahreiss, L., Sarkar, S., Futter, M., Menzies, F.M. et al. (2011) Lysosomal positioning coordinates cellular nutrient responses. *Nat. Cell Biol.* **13**, 453–460 [CrossRef PubMed](#)
- 79 Ma, X., Liu, H., Murphy, J.T., Foyil, S.R., Godar, R.J., Abuirgeba, H., Weinheimer, C.J., Barger, P.M. and Diwan, A. (2015) Regulation of the transcription factor EB-PGC1alpha axis by beclin-1 controls mitochondrial quality and cardiomyocyte death under stress. *Mol. Cell Biol.* **35**, 956–976 [CrossRef PubMed](#)
- 80 Scott, I., Webster, B.R., Chan, C.K., Okonkwo, J.U., Han, K. and Sack, M.N. (2014) GCN5-like protein 1 (GCN5L1) controls mitochondrial content through coordinated regulation of mitochondrial biogenesis and mitophagy. *J. Biol. Chem.* **289**, 2864–2872 [CrossRef PubMed](#)
- 81 Taniguchi, M., Nadanaka, S., Tanakura, S., Sawaguchi, S., Midori, S., Kawai, Y., Yamaguchi, S., Shimada, Y., Nakamura, Y., Matsumura, Y. et al. (2015) TFE3 Is a bHLH-ZIP-type Transcription Factor that Regulates the Mammalian Golgi Stress Response. *Cell Struct. Funct.* **40**, 13–30 [CrossRef PubMed](#)
- 82 Chen, Y., Azad, M.B. and Gibson, S.B. (2009) Superoxide is the major reactive oxygen species regulating autophagy. *Cell Death Differ* **16**, 1040–1052 [CrossRef PubMed](#)
- 83 Giordano, S., Darley-Usmar, V. and Zhang, J. (2014) Autophagy as an essential cellular antioxidant pathway in neurodegenerative disease. *Redox Biol* **2**, 82–90 [CrossRef PubMed](#)
- 84 Elzi, D.J., Song, M., Hakala, K., Weintraub, S.T. and Shio, Y. (2014) Proteomic analysis of the EWS-Fli-1 interactome reveals the role of the lysosome in EWS-Fli-1 turnover. In *J. Proteome Res.*, in the press
- 85 Polito, V.A., Li, H., Martini-Stoica, H., Wang, B., Yang, L., Xu, Y., Swartzlander, D.B., Palmieri, M., di Ronza, A., Lee, V.M. et al. (2014) Selective clearance of aberrant tau proteins and rescue of neurotoxicity by transcription factor EB. *EMBO Mol. Med.* **6**, 1142–1160 [CrossRef PubMed](#)
- 86 Martina, J.A. and Puertollano, R. (2013) Rag GTPases mediate amino acid-dependent recruitment of TFEB and MITF to lysosomes. *J. Cell Biol.* **200**, 475–491 [CrossRef PubMed](#)

Received 22 May 2014/08 June 2015; accepted 11 Jun 2015

Published as BJ Immediate Publication 11 June 2015, doi:10.1042/BJ20140645